Rare Metal Materials and Engineering
Volume 46, Issue 2, February 2017
Online English edition of the Chinese language journal

Available online at www.sciencedirect.com
ScienceDirect

Cite this article as: Rare Metal Materials and Engineering, 2017, 46(2): 0301-0306.

ARTICLE

Fabrication and Cyclic Oxidation of Y_2O_3/CeO_2-Modified Low Temperature Aluminide Coatings

Zhang Haijun, Sun Jianfeng

Heilongjiang University of Science and Technology, Harbin 150022, China

Abstract: With Y_2O_3/CeO_2 powder, instead of part of Al_2O_3, acting as filler, Y_2O_3/CeO_2-modified aluminide coatings were produced on Ni based using a conventional pack-cementation method at 600 ℃ for 10 h. For comparison, a normal aluminide coating was also produced using pure Al_2O_3 acting as filler. Effect of Y_2O_3/CeO_2 in the pack on the alumina phase transformation and cyclic oxidation resistance in air at 1000 ℃ was investigated. The results indicate that Y_2O_3 and CeO_2 have different effects on θ-α phase transformation: Y_2O_3 suppresses the growth of the θ-alumina but CeO_2 promotes the θ-α phase transformation. However, compared to the normal aluminide coating, the addition of Y_2O_3/CeO_2 significantly improves the cyclic oxidation resistance due to the formation of adherent alumina scale, especially the later. The effects of Y_2O_3/CeO_2 on alumina phase transformation and cyclic oxidation resistance were discussed.

Key words: aluminide; cyclic oxidation; reactive element effect

The addition of reactive element (RE), such as Y, Ce, and La, or reactive-element oxide (REO), such as Y_2O_3, CeO_2, La_2O_3, can improve the oxidation resistance of alloys, which was referred to as "reactive element effect" (REE) [1]. Various theories to elucidate the REE have been put forward but still are in dispute [2]. A large number of research has developed this effect of REO addition into the aluminide coating through depositing on the surface of alloy by various techniques before aluminization[3-6]. However, these methods not only complicated their technologic steps, but also added to the difficulty in preparation of these modified coatings. It was well known that the filler Al_2O_3 particles could be entrapped into the outer layer of aluminide coating[7, 8]. By considering this phenomenon, Zhou et al. [9] developed a much simpler technologic process to add Y_2O_3 particles into the aluminide coatings by the Y_2O_3 microparticles instead of part of Al_2O_3 as filler at 1000 ℃. Zhao[10] further investigated the effect of Y_2O_3 content in the filler on microstructure and hot corrosion resistance of aluminide coating produced at 1050 ℃. However, such a high temperature treatment inevitably restrict the applications of aluminide coatings due to grain growth of the substrate materials, which has a detrimental effect on the mechanical properties of workpieces. Therefore, reducing pack cementation temperature is required for the widespread application of the aluminide coatings[4-6]. Recently, Sun et al[11] successfully added CeO_2 nanoparticles into the chromizing coatings using the same methods at low temperature. Meng et al [12] further found that the chromizing coating using part of CeO_2 as filler exhibits better oxidation resistance than the chromizing coatings using pure Al_2O_3/CeO_2 as filler. The authors work[13] also indicated that Y_2O_3/CeO_2 can be added into aluminide coating using part of Y_2O_3/CeO_2 as filler at 600 ℃. Oxidation results showed that Y_2O_3/CeO_2 significantly enhanced the isothermal oxidation resistance of aluminide coatings. Based on these studies, the objective of the present work was to analyze the effect of Y_2O_3/CeO_2 on alumina phase transformation and cyclic oxidation resistance of aluminide coatings.

1 Experiment

Received date: February 14, 2016
Foundation item: Scientific Research Fund of Heilongjiang Provincial Education Department (11531319)
Corresponding author: Zhang Haijun, Ph. D., Associate Professor, College of Materials Science and Engineering, Heilongjiang University of Science and Technology, Harbin 150022, P. R. China, Tel: 0086-451-88036740, E-mail: kjdx1@163.com

Samples with dimensions of 15 mm×10 mm×2 mm were cut from an electrolytic nickel plate. They were ground to a final 800# SiC paper. After ultrasonically cleaning in acetone, they were aluminized using conventional pack cementation in a homogeneous mixture of 75 wt%Al powder as master alloy source, 20 wt% inert filler (namely 100 wt% Al_2O_3, 50 wt% Y_2O_3 (40~50 nm) + 50 wt% Al_2O_3 and 50 wt% CeO_2 (40~50 nm) +50 wt% Al_2O_3, respectively) and 5 wt% NH_4Cl as activator in a pure Ar atmosphere at 800 ℃ for 7 h. Afterwards, the samples were brushed, cleaned in bubbling distilled water for 30 min and then ultrasonically cleaned in acetone to remove any loosely embedded pack particles. The details and processing parameters were reported in Ref.[13].

The cyclic oxidation at 1000 ℃ up to 40 h in air was performed by automatically lifting samples from the hot zone of a vertical furnace after an 1 h exposure period followed with 10 min cooling to room temperature. Mass changes of the oxidized specimens were measured after fixed time intervals using a balance with 0.01 mg sensitivity. The composition and phases of the various aluminide coatings before and after oxidation was investigated using Camscan MX2600FE type scanning electron microscopy (SEM) with energy dispersive X-ray analysis (EDAX), transmission electron microscopy (TEM) and D/Max-2500pc type X-ray diffraction (XRD). Electroless Ni-plating was plated on the surface of the oxidized specimens to prevent the spallation of the scales for observing cross-sections.

2 Results

2.1 Microstructure

After pack cementation at 600 ℃ for 10 h, the aluminide coatings were prepared. Previous results indicated that the addition of Y_2O_3 or CeO_2 in the pack significantly retarded the grain growth of the aluminide coating [13]. The average Al concentration in the surface zone (<4 μm: the profile depth of electron beam) is close to 41 wt% for the three aluminide coatings on a basis of EDAX area analysis. XRD results also reveal that all aluminide coatings contain only δ-Ni_2Al_3 phase, as seen in Fig.1.

Fig.2 shows the corresponding cross-sectional morphologies of δ-Ni_2Al_3 coatings developed on Ni using different filler. Clearly, the aluminide coatings using part of Y_2O_3 or CeO_2 as filler is more compact than the aluminide coating using pure Al_2O_3 as filler even all have the same thickness about 50 μm. From Fig.2a, it can be found that there is a 2~3 μm interdiffusion zone (as arrowed). However, for aluminide coatings using Y_2O_3/CeO_2 as filler, the thickness of interdiffusion zone is significantly decreased, especially the later. No bright Y_2O_3/CeO_2-oxides particles can be found from Fig.2b and Fig.2c. The result is contrary to Zhou [9] but the same as other works [10-12] using finer Y_2O_3/CeO_2 particles as filler.

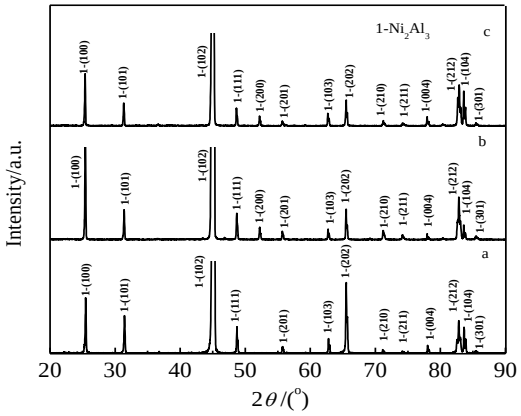

Fig.1 XRD patterns of aluminide coatings using different filler (a-Al_2O_3, b-Al_2O_3+Y_2O_3, c-Al_2O_3+CeO_2)

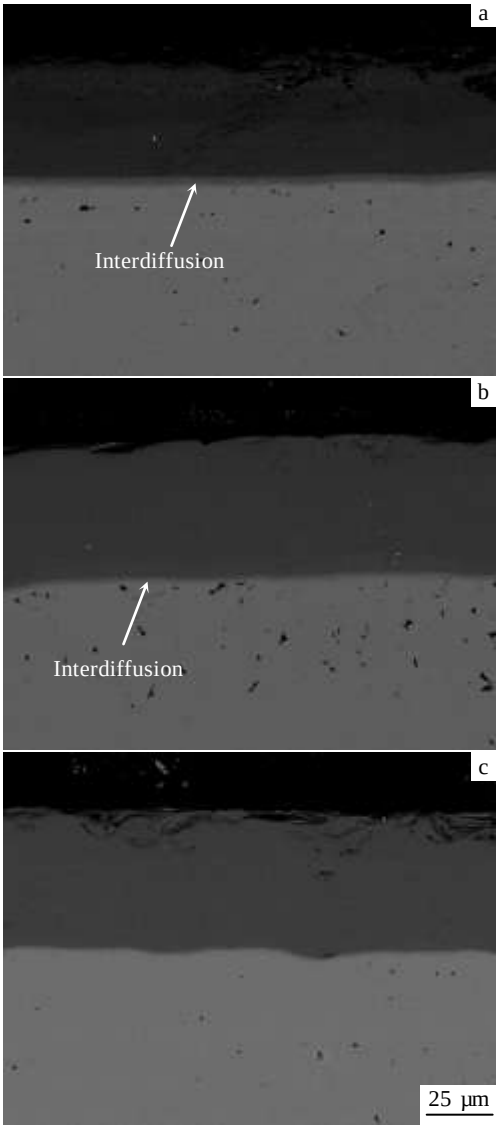

Fig.2 Cross sectional morphologies of aluminide coatings using different filler: (a) Al_2O_3, (b) Al_2O_3+Y_2O_3, and (c) Al_2O_3+CeO_2

Fig.3 shows bright-field images of the three δ-Ni_2Al_3 coatings. The mean grain size of the normal aluminide without CeO_2 or Y_2O_3 particles is 1~2 μm, as seen in Fig.3a, whereas the value is reduced to 600~700 nm for the Y_2O_3-modified aluminide and to 400~500 nm for the CeO_2-modified aluminide, as seen in Fig.3b and Fig.3c. Furthermore, it is clear that near the CeO_2/Y_2O_3 particles or its clusters (as arrowed), finer grain occurs, indicating that the grain growth of the δ-Ni_2Al_3 is retarded by the dispersed CeO_2 or Y_2O_3 particles.

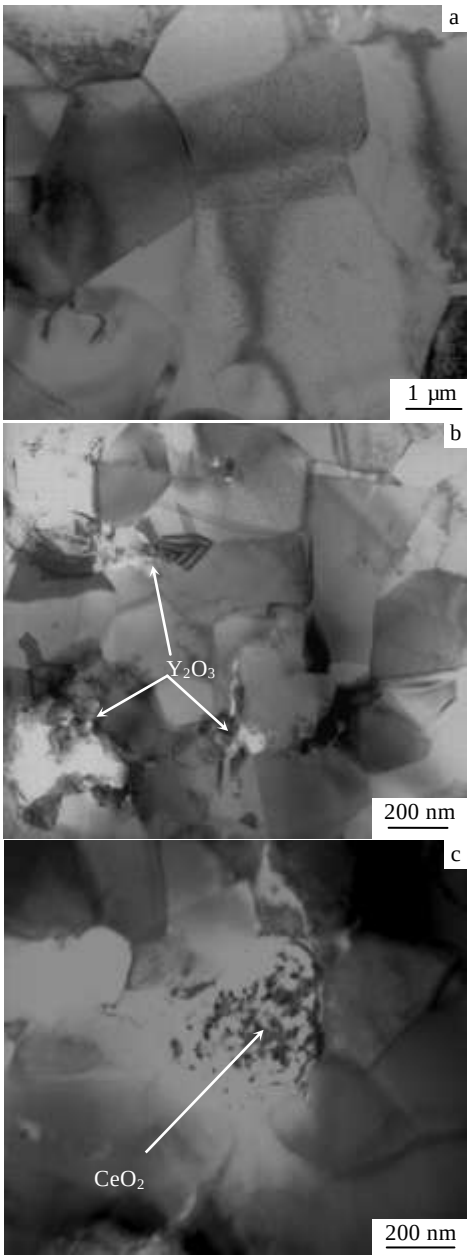

Fig.3 TEM images of the aluminide coatings close to surface areas using different filler: (a) Al_2O_3, (b) Al_2O_3+Y_2O_3, and (c) Al_2O_3+CeO_2

2.2 Cyclic-oxidation

Fig.4 illustrates the mass change vs. time curves of cyclic oxidation of the various aluminide coatings in air at 1000 ℃ (the mass loss by spallation is not considered). For the normal aluminide coating, significant mass loss occurs at 20 cycles, due to severe spallation which could be seen by the naked eye. Occasionally an approach of the mass by spallation to that by oxidation leads to no obvious mass change during the cyclic number from 25 to 40. In contrast, the oxidation rate of the Y_2O_3/CeO_2-modified aluminide coatings steadily decreases, and the scale spallation does not occur, especially the later. From Fig.4, it can be found that the scales formed on Y_2O_3/CeO_2 modified aluminide coatings are profoundly oxidation resistant.

All aluminide coatings after 40 h cyclic oxidation were characterized using XRD and the results are presented in Fig.5. The results indicate that both normal aluminide coatings and Y_2O_3-modified aluminide coating grow a protective scale of alumina in it's α and θ forms. However, only α-Al_2O_3 is detected on the CeO_2 modified-aluminide coating. From Fig.5, it can be also found that the phase of normal aluminide coating after cyclic oxidation is Ni_3Al with minor $Ni_{0.9}Al_{1.1}$. In contrast, the aluminide coatings using Y_2O_3/CeO_2 as filler still maintain $Ni_{0.9}Al_{1.1}$ phase, suggesting Y_2O_3/CeO_2 significantly delays the degradation of aluminide coatings.

To clarify the difference in the oxidation performance of various aluminide coatings, surface and cross-sectional morphologies of the scales formed were investigated.

Fig.6 reveals the SEM top-views of the scales formed on various aluminide coatings after 40 h exposure in air at 1000 ℃. Blocky scale spallation is visible on the normal aluminide coatings, as seen in Fig.6a. From the corresponding magnified image in Fig.6b, whisker- and needle-like oxide crystals appear. These crystals are the alumina in its θ phase form, as has been characterized by XRD. For Y_2O_3/CeO_2-modified aluminide coatings, no spallation

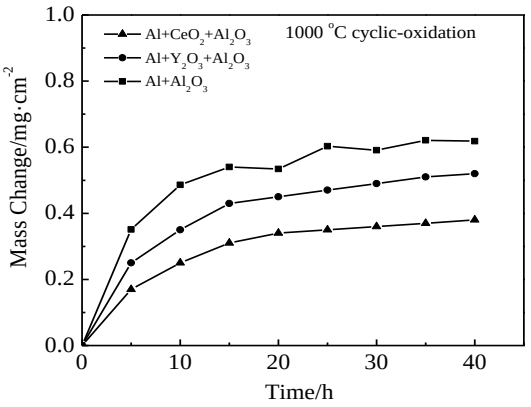

Fig.4 Cyclic oxidation curves of aluminide coatings using different filler in air at 1000 ℃ for 40 h

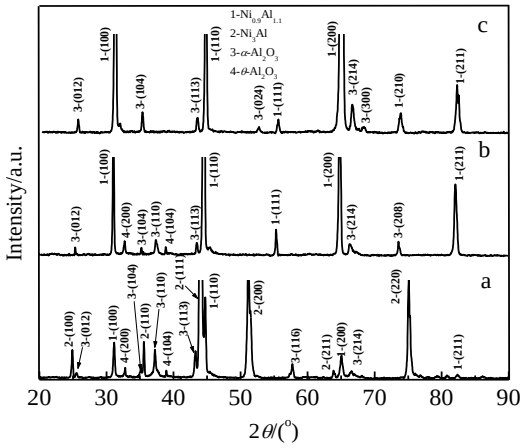

Fig.5 XRD patterns of aluminide coatings after cyclic-oxidation at 1000 ℃ for 40 h using different filler (a-Al_2O_3, b-Al_2O_3+Y_2O_3 and c-Al_2O_3+CeO_2)

occurs as seen from Fig.6c and Fig.6e. From Fig.6d, shorter whisker- and needle-like θ alumina scale with crack appears on the Y_2O_3-modified aluminide coatings, suggesting that Y_2O_3 suppresses the growth of the θ-alumina. However, only round α-Al_2O_3 appears on the CeO_2-modified aluminide coatings, as seen in Fig.6f, suggesting that CeO_2 accelerates the θ-α phase transformation.

From the corresponding cross sections of the oxide scale, it could be found that a thicker scale with significant voids, cracking and delamination is formed on the normal aluminide coating, as seen in Fig.7a. However, for Y_2O_3/CeO_2-modified aluminide coatings, thinner scales with only voids could be observed, as seen in Fig.7b and Fig.7c. At the same time, the growth of θ-Al_2O_3 on the normal aluminide coating and Y_2O_3-modified aluminide coatings can also be confirmed from Fig.7a and Fig.7b, where the θ-Al_2O_3 whiskers formed on the top of the scale is visible.

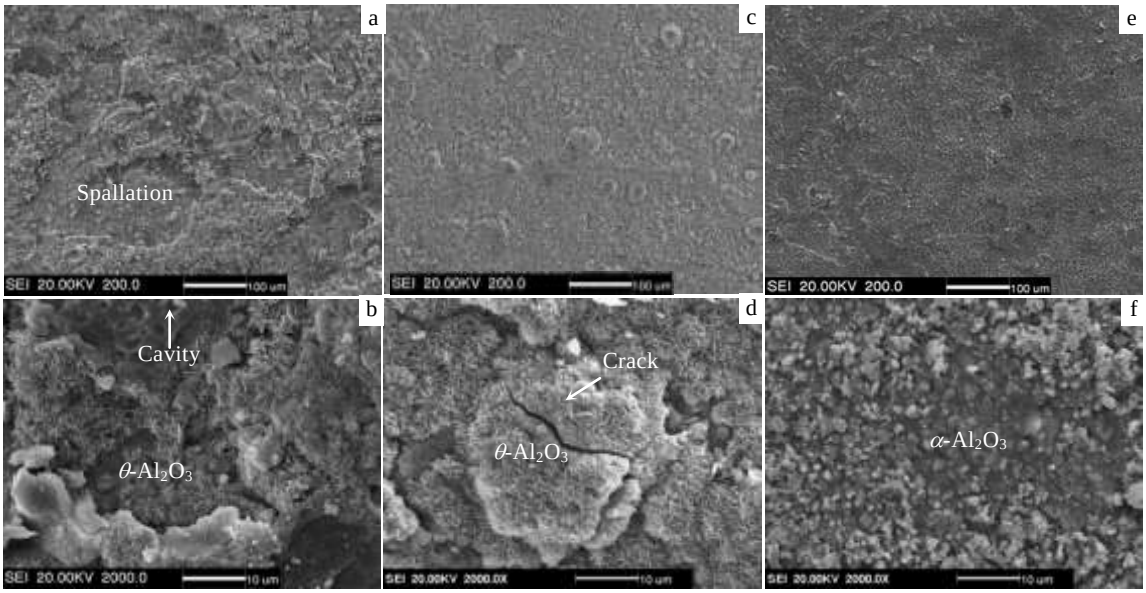

Fig.6 Surface morphologies of the oxide scales formed on aluminide coatings using different filler: (a, b) Al_2O_3, (c, d) Al_2O_3+Y_2O_3, and (e, f) Al_2O_3+ CeO_2

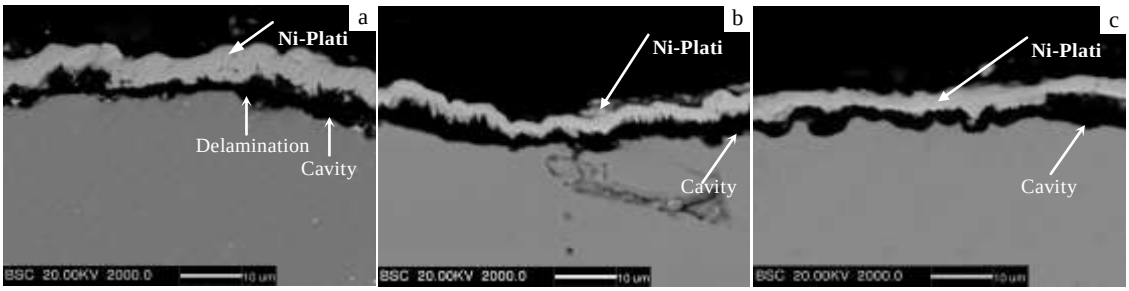

Fig.7 Cross-sectional morphologies of the oxide scales formed on aluminide coatings using different filler: (a) Al_2O_3, (b) Al_2O_3+Y_2O_3, and (c) Al_2O_3+ CeO_2

3 Discussion

Previous results [4-6] indicated that δ-Ni_2Al_3 coatings normally forms whisker- and needle-like θ-Al_2O_3 during the short transient oxidation stage due to high Al content. The whisker-like θ-Al_2O_3 has high density of twins acting as a fast transport path for Al cation during oxidation. Previous results[14,15] also indicated that θ-alumina appears in the outer part of the scale and α-alumina in the area close to the scale/metal interface. For Y_2O_3/CeO_2-modified aluminide coatings, the formation of alumina will sweep Y_2O_3/CeO_2 nanoparticles at/adjacent to the surface. After being incorporated into the growing scale, Y or Ce ions from Y_2O_3/CeO_2 nanoparticles in the alumina scale segregate to the scale grain-boundaries and then transport outwards, driven by the oxygen potential gradient between the interfaces of the metal/scale and the scale/gas [16]. In this case, a different effect [3-9, 14-18] on the θ-α transformation occurred. In this experiment, Y significantly hinders the outward short-circuit diffusion of the Al for the growth of the θ-alumina, thus a lower oxidation rate with shorter θ-alumina whiskers being observed. As it is further oxidized, θ-Al_2O_3 will gradually convert into a round shape α-Al_2O_3, which is a thermodynamically stable phase and is slow-growing. If the θ-α phase transformation completes quickly, the tensile stresses induced by the volume contraction (13.4%) may be large enough to give rise to cracks (Fig.6d) and spallation (Fig.6a) in the growing scale. However, for CeO_2-modified aluminide coating, only round α-Al_2O_3 can be observed. The result indicates that Ce accelerates the θ-α transformation.

The spallation was inherently correlated with the formation of large interface cavities, as having been extensively reported elsewhere [19-21]. Generally speaking, the interface cavities form as a result of condensation of cation vacancies injected from the growing alumina scale for counterbalancing the outward cation diffusion or from the coating due to ‘‘Kirkendall” effect pertinent to the relative diffusion rate of nickel to aluminum toward the coating interior during oxidation. The formation of large interface cavities greatly decreases the critical stress (δ_c) for scale decohesion according to the equation: $\delta_c=K_{IC}/(\pi c)^{1/2}$ [22], where K_{Ic} is the critical stress intensity factor and c a half length of interface defect. The spallation mainly occurs during cooling, due to the large thermal stress generated during cooling as a consequence of mismatching coefficients of thermal expansion between the alumina scale and the coating. The scale cracking and spallation exposes the underlying coating directly to the air during the subsequent oxidation, as seen in Fig.6a. In contrast, no spallation and less interface voids occur on the CeO_2/Y_2O_3 modified aluminide coating. On this basis, it is assumed that the addition of CeO_2/Y_2O_3 evidently enhances the adherence of the scale. The relative reasons are interpreted as follows: 1) CeO_2/Y_2O_3 refines the grains of aluminide coating [13], which significantly increases sites for aluminia nucleating from the onset of oxidation, leading to the development of finer-grained adherent alumina scale; 2) CeO_2/Y_2O_3 significantly decreases the oxidation rates, leading to a reduction of the interface voiding kinetics; 3) Ce/Y ion or its precipitates pinned the scale-grain boundaries [23], leads to the formation of fine-grained scales with enhanced adhesion; 4) CeO_2/Y_2O_3 particles favor to enhance the adhesion of the scale, by acting as sinks for vacancies condensation to prevent the large interface cavity formation[4-6,10-19,24] and by scavenging the interface sulfur [25,26].

Heavy spallation and higher oxidation rate due to the formation of θ-Al_2O_3 completely convert the normal aluminide (Ni_2Al_3 phase) coating into Ni_3Al with minor $Ni_{0.9}Al_{1.1}$. However, the addition Y_2O_3/CeO_2 significantly decreases the oxidation rate and improves the cyclic oxidation resistance, as addressed above, which significantly delays the degradation of aluminide coatings. This is the reason why it still retains $Ni_{0.9}Al_{1.1}$ phase, as seen from Fig.5.

Taking into account the results in this work, we believe that the methods may be extended to other alloys. Aluminized coatings with a desired oxidation performance may be fabricated at further decreased temperatures. Hence, the one-step process represents a novel route of manufacturing a low-temperature aluminized coating capable of thermally forming a compact, continuous alumina scale.

4 Conclusions

1) Using part of Y_2O_3/CeO_2, instead of partial Al_2O_3, acting as the filler, the Y_2O_3/CeO_2 is successfully entrapped into the aluminide coating.

2) Y_2O_3 suppresses the growth of θ-alumina, but CeO_2 accelerates the θ to α-alumina transformation.

3) The addition of Y_2O_3/CeO_2 significantly improves the cyclic oxidation resistance due to the formation of adherent alumina scale.

References

1 Pfeil L B. *UK Patent*, 459848[P]. 1937

2 Moon D P. *Mater Sci Tech*[J], 1989, 5: 754

3 Chevalier S, Nivot C, Larpin J P. *Oxidation of metals*[J], 2004, 61: 195

4 Xu C, Peng X and Wang F. *Corrosion Science*[J], 2010, 52: 740

5 Peng X, Guan Y, Dong Z, Xu C and Wang F. *Corrosion Science* [J], 2011, 53: 1954

6 Zhou Y B, Hu H T, Zhang H J. *Vacuum*[J], 2011, 86: 210

7 Goward G W and Boone D H. *Oxidation of Metals*[J], 1971, 3: 475

8 Xiang Z D and Datta P K. *Journal of Materials Science*[J], 2003, 38: 3721
9 Zhou W, Zhao Y G, Li W *et al*. *Materials Science and Engineering*[J], 2007, 458A: 34
10 Zhao X S, Zhou C G. *Corrosion science*[J], 2014, 86: 223
11 Sun J F, Zhou Y B, Zhang H J. *Transactions of Nonferrous Metals Society of China* [J], 2013, 23: 1375
12 Meng J S, Ji Z S. *Transactions of Nonferrous Metals Society of China* [J], 2014, 24: 1785
13 Zhang Haijun, Sun Jianfeng. *Rare Metal Materials and Engineering*[J], 2015, 44(11): 2628
14 Schumann E. *Oxidation of Metals*[J], 1995, 43: 157
15 Yang J C, Schumann E, Levin I *et al*. *Acta Materialia*[J], 1998, 46: 2195
16 Pint B A and Hobbs L W. *Oxidation of Metals*[J], 1996, 45: 1
17 Burtin P, Brunelle J P, Puolat M *et al*. *Applied Catalysis*[J], 1987, 34: 225
18 Kitajima Y, Hayashi S, Nishimoto T *et al*. *Oxidation of Metals*[J], 2011, 75: 41
19 Brumm M W, Grabke H J. *Corrosion Science*[J], 1993, 34: 547
20 Hou P Y, Priimak K. *Oxidation of metals*[J], 2005, 63: 113
21 Peng X, Li M, Wang F. *Corrosion science*[J], 2011, 53: 1616
22 Hancock P and Nicholls J R. *Mater Sci Technol*[J], 1988, 4: 398
23 Hindam H M, Whittle D P. *J Electrochem Soc*[J], 1982, 129: 1147
24 Kumar A, Nasrallah M M, Douglass D L. *Oxidation of Metals* [J], 1974, 8: 227
25 Kuenzly J D, Douglass D L. *Oxidation of Metals*[J], 1974; 8:139
26 Lees D G. *Oxidation of Metals*[J], 1987, 27: 75

Y_2O_3/CeO_2 改性的低温渗铝涂层制备和循环氧化性能研究

张海军，孙俭峰
(黑龙江科技大学，黑龙江 哈尔滨 150022)

摘 要：利用Y_2O_3/CeO_2纳米颗粒替代部分Al_2O_3粉作为填充剂，在Ni基体上, 600 ℃低温渗铝10 h，制备了Y_2O_3/CeO_2改性的低温渗铝涂层。作为对比，采用相同的工艺在Ni基体上利用纯Al_2O_3粉制备了普通渗铝涂层。对比研究了Y_2O_3/CeO_2是如何影响氧化铝的相变以及渗铝涂层的1000 ℃时的循环氧化性能。结果发现，Y_2O_3和CeO_2对θ-α相变具有不同的作用：Y_2O_3抑制θ-Al_2O_3的长大，而CeO_2促进θ-α相变。与普通渗铝涂层相比，Y_2O_3/CeO_2改性的渗铝涂层形成粘附性更好的氧化铝膜，提高了渗铝涂层的循环氧化性能。文中对Y_2O_3/CeO_2是如何影响θ-α相变以及渗铝涂层的循环氧化性能进行了分析。

关键词：铝化物；循环氧化；活性元素效应

作者简介：张海军，男，1978 年生，博士，副教授，黑龙江科技大学材料科学与工程学院，黑龙江 哈尔滨 150022，电话：0451-88036740, Fax: 0451-88036219, E-mail: kjdx1@163.com